Limits of Plasma Oxidation in Cr_2O_3 ALD: Over-Oxidation, Etching, and Defect Control

S. Das[1], H. Yang[2], S. R. C. McMitchell[3], R. L. Peterson[2]

[1] imec USA, 3520 Green Court, Ann Arbor, [2] Department of Electrical Engineering and Computer Science, University of Michigan, 1301 Beal Ave, Ann Arbor, MI, 48109-2122, [3] imec Belgium, Kapeldreef 75, Leuven 3001, Belgium

p-type oxides are a critical missing component for CMOS-compatible oxide electronics and low-temperature memory integration. Cr_2O_3 is a promising p-type oxide due to its chemical stability, wide bandgap, and strong sensitivity of electronic properties to oxidation chemistry. However, reported hole mobilities span a wide range (~0.1 to 5–10 $cm^2/V \cdot s$),[1, 2] indicating that defects, particularly oxygen vacancies and growth conditions determine defects, film density and impurities which dominate transport. Plasma-enhanced atomic layer deposition (PE-ALD) offers a scalable, low-temperature pathway to precisely control oxidation chemistry and defect formation, as demonstrated in oxides such as HfO_2[3] and NiO[4, 5]. Despite this potential, PE-ALD of Cr_2O_3 has not been systematically explored. In this work, we directly compare ozone-based and oxygen plasma-based ALD of Cr_2O_3 to understand how plasma oxidation influences stoichiometry, defect density, and electronic quality.

Cr_2O_3 growth proceeds via ligand exchange between surface –OH groups and $Cr(acac)_3$. Ozone promotes combustion-like oxidation, while oxygen plasma supplies highly reactive O*, O_2^+, and OH species[6] that enable efficient ligand removal at lower temperatures but may also induce over-oxidation and etching. To isolate plasma effects, we first establish a well-controlled ozone-ALD baseline. Systematic optimization of ozone dose, metal precursor dose, and temperature reveals a narrow growth window: the growth rate saturates with Cr dose, it increases and then decreases with ozone exposure due to over-oxidation, and it increases with temperature until volatile CrO_3[7] formation dominates. Grazing Incidence X-ray Diffraction (GIXRD) confirms that this window yields crystalline, phase-stable Cr_2O_3.

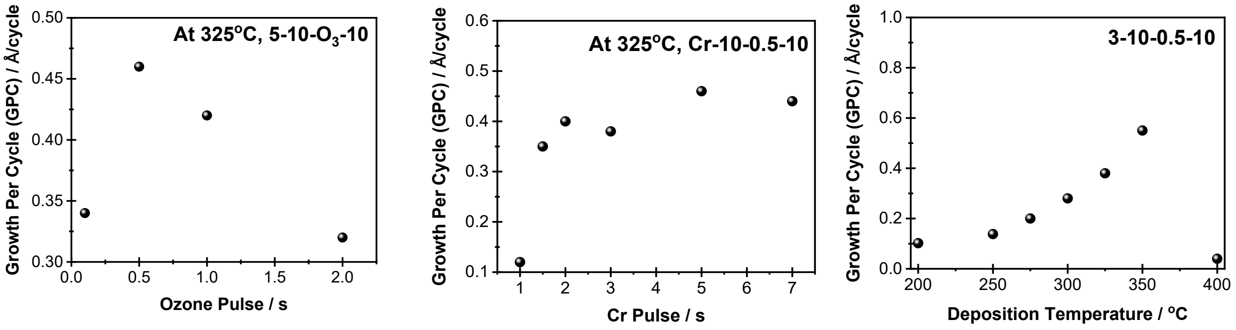

Figure 1: Optimization of ozone-ALD Cr_2O_3 deposition conditions.

We then transition to PE-ALD at 250 °C. Under aggressive O_2 plasma conditions, net film growth is strongly suppressed, indicating concurrent over-oxidation ($Cr^{3+} \rightarrow Cr^{6+}$) and plasma-induced etching, likely associated with the formation of volatile CrO_3 species. AFM analysis reveals highly rough and non-uniform surfaces, consistent with plasma damage and/or poor nucleation. While reducing the oxidant dose partially restores growth, the process remains highly sensitive to plasma power and continues to suffer from significant surface roughness. These observations highlight a central challenge in PE-ALD of Cr_2O_3: stabilizing the Cr^{3+} oxidation state while suppressing plasma-induced etching to achieve smooth, uniform films with measurable net growth.

Ongoing work therefore prioritizes mitigation of plasma-induced etching through plasma power optimization and process stabilization, as a prerequisite to further oxidant dose tuning. Establishing a viable PE-ALD process window with controlled oxidation and acceptable morphology will enable subsequent evaluation of the films' electrical properties via Hall measurements and thin-film transistor fabrication, and correlation with oxidant chemistry, process conditions, and defect density. Overall, this study provides critical insight into the limits and opportunities of plasma oxidation for p-type oxide ALD and establishes a framework for defect-engineered Cr_2O_3 targeting CMOS-compatible memory technologies.

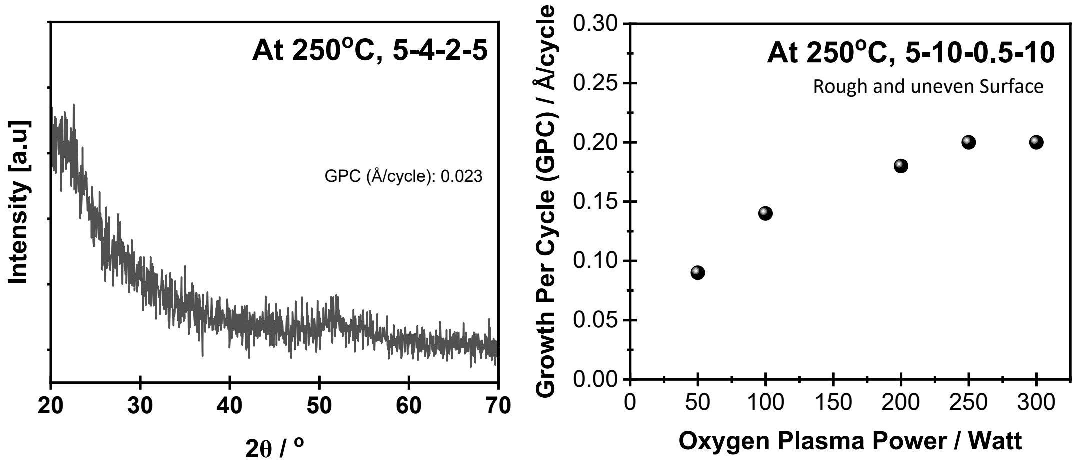

Figure 2: Higher plasma dose leads to negligible growth; thus, plasma generation power optimization needed to maximize growth and minimize etching

References:

[1] Appl Phys Lett, 99, 11, **2011**
[2] Mater Res Express, 11, 10, **2024**
[3] Materials Science and Engineering: B, 285, 115964, **2022**
[4] Applied Physics Letters,121, 11, 111603, **2022**
[5] ACS Omega, 10, 1, 422–438, **2025**
[6] Applied Surface Science, 75, 1–4, 220–227, **1994**
[7] J. Vacuum Science & Technology A, 39, 3, 032414, **2021**